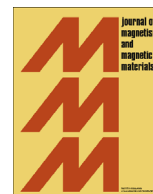




ELSEVIER

Contents lists available at ScienceDirect

## Journal of Magnetism and Magnetic Materials

journal homepage: [www.elsevier.com/locate/jmmm](http://www.elsevier.com/locate/jmmm)

## Processing of alnico permanent magnets by advanced directional solidification methods

Min Zou<sup>a,\*</sup>, Francis Johnson<sup>a</sup>, Wanming Zhang<sup>a</sup>, Qi Zhao<sup>a</sup>, Stephen F. Rutkowski<sup>a</sup>, Lin Zhou<sup>b,c</sup>, Matthew J. Kramer<sup>b,c</sup><sup>a</sup> Ceramic and Metallurgy Technologies, General Electric Global Research, Niskayuna, NY, United States<sup>b</sup> Ames Laboratory, Ames, IA, United States<sup>c</sup> Iowa State University, Ames, IA, United States

## ARTICLE INFO

## Article history:

Received 23 May 2016

Received in revised form

24 June 2016

Accepted 29 June 2016

Available online 5 July 2016

## Keywords:

Alnico

Directional solidification

Permanent magnets

Transmission electron microscopy

## ABSTRACT

Advanced directional solidification methods have been used to produce large (> 15 cm length) castings of Alnico permanent magnets with highly oriented columnar microstructures. In combination with subsequent thermomagnetic and draw thermal treatment, this method was used to enable the high coercivity, high-Titanium Alnico composition of 39% Co, 29.5% Fe, 14% Ni, 7.5% Ti, 7% Al, 3% Cu (wt%) to have an intrinsic coercivity ( $H_{ci}$ ) of 2.0 kOe, a remanence ( $B_r$ ) of 10.2 kG, and an energy product  $(BH)_{max}$  of 10.9 MGOe. These properties compare favorably to typical properties for the commercial Alnico 9. Directional solidification of higher Ti compositions yielded anisotropic columnar grained microstructures if high heat extraction rates through the mold surface of at least 200 kW/m<sup>2</sup> were attained. This was achieved through the use of a thin walled (5 mm thick) high thermal conductivity SiC shell mold extracted from a molten Sn bath at a withdrawal rate of at least 200 mm/h. However, higher Ti compositions did not result in further increases in magnet performance. Images of the microstructures collected by scanning electron microscopy (SEM) reveal a majority  $\alpha$  phase with inclusions of secondary  $\alpha_\gamma$  phase. Transmission electron microscopy (TEM) reveals that the  $\alpha$  phase has a spinodally decomposed microstructure of FeCo-rich needles in a NiAl-rich matrix. In the 7.5% Ti composition the diameter distribution of the FeCo needles was bimodal with the majority having diameters of approximately 50 nm with a small fraction having diameters of approximately 10 nm. The needles formed a mosaic pattern and were elongated along one  $\langle 001 \rangle$  crystal direction (parallel to the field used during magnetic annealing). Cu precipitates were observed between the needles. Regions of abnormal spinodal morphology appeared to correlate with secondary phase precipitates. The presence of these abnormalities did not prevent the material from displaying superior magnetic properties in the 7.5% Ti composition. Higher Ti compositions did not display the preferred spinodal microstructure, explaining their inferior magnetic properties.

© 2016 Elsevier B.V. All rights reserved.

## 1. Introduction

Alnico permanent magnets have attracted revived interest since the recent spike in rare earth element prices [1–5]. Stoner-Wohlfarth theory predicts a maximum energy product  $(BH)_{max}$  of 49 MGOe for a 67 vol% packed Fe<sub>65</sub>Co<sub>35</sub> nanostructure, given the FeCo nanowires do not exceed the coherence radius of the order of 10 nm [6]. The highest energy products achieved in Alnico permanent magnets, however, are 13.4 and 9.0 MGOe, in laboratory and commercial grades Alnico 9, respectively, with an intrinsic coercivity ( $H_{ci}$ ) of 1.5 kOe [7]. The highest  $H_{ci}$  in commercial Alnico is 2.2 kOe in Alnico 8H with an energy product of 5.0 MGOe [8]. The major difference between the Alnico 8H and 9 compositions is

that 8H has higher Co and Ti contents. It has been reported that high Ti content favors the high coercivity but impedes the formation of the columnar grain structure, thus degrading the remanence ( $B_r$ ) and energy product [7]. For example, the commercial Alnico 9 with a 5 wt% Ti has a columnar grain structure, but the Alnico 8H with a 7.5 wt% Ti is randomly grained [4]. The columnar grain structure has been reported in 7.5% Ti using the controlled cooling method with a speed of 5 mm/h [9], and in 8.2% Ti without disclosure of casting details [10]. No literature report can be found on successful casting of Ti composition higher than 8.2% with a columnar microstructure. This study explores the application of advanced directional solidification casting methods to 7.5% and higher Ti (9% and 12%) compositions in order to form highly oriented columnar microstructures to improve the  $B_r$  and energy products and maintain or improve the high  $H_{ci}$  in these compositions.

\* Corresponding author.

## 2. Experimental details

Master ingots of three compositions of Alnico were cast by vacuum induction melting. Three casts were prepared in an ALD VIM-IC liquid metal cooled vacuum investment casting furnace using molds with cavity dimensions of  $150 \times 38 \times 38 \text{ mm}^3$ . Liquid tin (Sn) was used as the coolant medium. The alloy compositions, mold parameters, and casting conditions are listed in Table 1.

The as-cast alloys were cut into  $15 \times 10 \times 2 \text{ mm}^3$  slices from the middle sections of the ingots. One slice for each composition was etched using Marble etchant (10 g  $\text{CuSO}_4$  in 50 ml  $\text{HCl} + 50 \text{ ml H}_2\text{O}$  solution) for a few seconds to reveal dendritic structures evaluated using the LEO 1450VP SEM and KEYENCE VHX-600 light microscope. Other slices were solution heat treated at different solutionization temperatures and time durations chosen as the ones to yield least secondary phase volume fractions based on the SEM data. The solutionized alloys were then cut into  $\approx 4 \times 2 \times 2 \text{ mm}^3$  parallelepipeds for thermomagnetic and draw cycle treatments in a magnetic field of 2.7 kOe applied along the columnar grain direction at different temperatures and time durations optimized for different alloy compositions exhibiting the highest  $H_{ci}$ . In particular, because the spinodal decomposition temperature of each alloy composition was unknown, the magnetothermal treatments were carried out first at an estimated spinodal decomposition temperature ( $T_1$ ) for 10 min, then at temperatures 20 °C higher ( $T_2$ ) and lower ( $T_3$ ) than  $T_1$ . The  $H_{ci}$  of the samples heat treated at these three temperatures were then measured. If the  $H_{ci}$  of the sample heat treated at  $T_2$  was greater than that at  $T_1$ , then the next heat treatment was set at a temperature 20 °C higher than  $T_2$ . If the  $H_{ci}$  of the sample heat treated at  $T_3$  was greater than that at  $T_1$ , then the next heat treatment was set at a temperature 20 °C lower than  $T_3$ . The  $H_{ci}$  of each sample after every heat treatment was measured and compared, until a highest  $H_{ci}$  was observed at a particular temperature ( $T_n$ ) for a specific alloy composition. Then the thermomagnetic treatments were carried out at temperatures 10 °C higher and lower than  $T_n$ . The  $H_{ci}$  of the two samples were compared, and the temperature at which yielded the highest  $H_{ci}$  was determined as the optimal thermomagnetic treatment temperature ( $T_o$ ) for the alloy composition. Then the same method was used to vary the heat treatment time between 1 and 120 min at  $T_o$  for each alloy composition. The two-step draw cycle treatments were also optimized between 500 and 675 °C and between 6 and 48 h in the same manner.

The magnetic properties of the heat treated samples were measured using a Quantum Design Physical Property

**Table 1**

Compositions, mold and casting conditions, and magnetic properties of the alnico alloys processed by directional solidification methods and subsequent magnetic field annealing.

| Sample ID            |         | 7.5% Ti  | 9% Ti    | 12% Ti   |
|----------------------|---------|----------|----------|----------|
| wt%                  |         |          |          |          |
|                      | Al      | 7        | 8        | 7        |
|                      | Ni      | 14       | 14       | 14       |
|                      | Fe      | 29.5     | 26.6     | 25.5     |
|                      | Co      | 39       | 39.4     | 39       |
|                      | Cu      | 3        | 3        | 3        |
|                      | Ti      | 7.5      | 9        | 12       |
| Face coat stucco     | Alumina | Alumina  | Alumina  | Alumina  |
| Backup stucco        | Alumina | Hi-K SiC | Hi-K SiC | Hi-K SiC |
| Shell thickness      | 5 mm    | 5 mm     | 5 mm     | 5 mm     |
| Melt temp. (°C)      | 1430    | 1430     | 1430     | 1430     |
| Withdraw rate (mm/h) | 152     | 203      | 203      | 203      |
| $M_s$ (kG)           | 11.0    | 9.2      | 8.7      | 8.7      |
| $B_r$ (kG)           | 10.2    | 5.4      | 4.0      | 4.0      |
| $H_{ci}$ (kOe)       | 2.0     | 2.2      | 1.3      | 1.3      |
| $(BH)_{max}$ (MGOe)  | 10.9    | 3.2      | 1.4      | 1.4      |

Measurement System (PPMS) Model 6000 equipped with a vibrating sample magnetometer (VSM). The demagnetization factors were corrected using the equation derived in [11] by cutting samples into rectangular specimens and carefully measuring their dimensions. The appropriately-corrected open-loop measurements were estimated to agree with closed-loop measurements to within  $\pm 3\%$  error [12].

Transmission electron microscopy (TEM) analysis was performed on transverse sections (with electron beam parallel to H direction) and on longitudinal orientation (with electron beam perpendicular to H direction) on a FEI Tecnai F20. TEM samples were prepared by mechanical wedge-polishing followed by a short time, low voltage Ar ion-milling with liquid nitrogen cold stage.

## 3. Results and discussion

The columnar grained microstructures are clearly evident in the optical images of the three alloys as shown Fig. 1.

For 1-D steady state directional solidification (DS), the liquid thermal gradient  $G_L$  is expected to increase as the melt temperature  $T_{melt}$  decrease, based on the heat balance equation,

$$G_L = \frac{k_S G_S - \rho_{melt} [H_f + C_{p,melt} (T_{melt} - T_L)] R}{k_L} \quad (1)$$

where  $G_L$  and  $G_S$  are liquid and solid thermal gradients at the liquid-solid interface,  $k_S$  and  $k_L$  are liquid and solid metal thermal conductivities,  $\rho_{melt}$  and  $C_{p,melt}$  are melt density and specific heat,  $T_L$  and  $H_f$  are alloy liquidus temperature and latent heat, and  $R$  the liquid-solid interface growth rate [13]. At a given solidification rate, a higher  $G_L$  enhances DS growth in the  $\langle 001 \rangle$  direction, which is coincident with Alnico easy direction for magnetization. The higher the  $G_L$  is, the lower the misorientation and the stronger the  $\langle 001 \rangle$  texture is.

Replacing solid heat flux  $k_S G_S$  with DS heat extraction rate,  $Q_{DS}$ , Eq. (1) can be rewritten as Eq. (2),

$$G_L = \frac{Q_{DS} - \rho_{melt} [H_f + C_{p,melt} (T_{melt} - T_L)] R}{k_L} \quad (2)$$

For given casting design and withdraw rate  $V$  for a given alloy,  $G_L$  increases as  $Q_{DS}$  increases and  $T_{melt}$  decreases. If assuming steady state growth and constant thermal boundary conditions,  $Q_{DS}$  as a function of withdrawal length  $L$ , can then be expressed in Eqs. (3), (3a), and (4)

$$Q_{DS}(L) = \frac{q_{z,0} [T_m(L) - T_{chill}]}{[T_s - T_{chill}]} + \frac{2(W + D)}{WD} \int_0^{L=Vt} q_{ex}(z) dz \quad (3)$$

$$Q_{DS}(L) = \frac{q_{z,0} [T_m(L) - T_{chill}]}{[T_s - T_{chill}]} + \frac{1}{m_c} \int_0^{L=Vt} q_{ex}(z) dz \quad (3a)$$

$$q_{ex} = h_{eff}(L) [T_{m,surf}(L) - T_{amb}] \quad (4)$$

where  $q_{z,0}$  is initial heat flux through casting/mold support interface in withdrawal direction,  $T_m(L)$  is casting temperature at mold support contact interface,  $T_{chill}$  is mold support temperature,  $T_s$  is solidus temperature,  $W$  and  $D$  are width and thickness of the DS ingot,  $q_{ex}$  is heat extraction rate normal to the vertical shell surface,  $m_c$  is casting modulus (volume to surface ratio),  $t$  is withdrawal time,  $h_{eff}$  is an effective heat transfer coefficient,  $T_{m,surf}$  is metal surface temperature, and  $T_{amb}$  is surrounding environment temperature. With certain approximations,  $h_{eff}$  in Eq. (4) can be

Download English Version:

<https://daneshyari.com/en/article/1797711>

Download Persian Version:

<https://daneshyari.com/article/1797711>

[Daneshyari.com](https://daneshyari.com)